

Gaussian Processes with Input Location Error and Applications to the Composite Parts Assembly Process

Wenjia Wang^{a,1}, Xiaowei Yue^b, Benjamin Haaland^{c,2}, C. F. Jeff Wu^{d,*}

^aThe Statistical and Applied Mathematical Sciences Institute

^bVirginia Polytechnic Institute and State University

^cUniversity of Utah

^dGeorgia Institute of Technology

Abstract

In this paper, we investigate Gaussian process regression with input location error, where the inputs are corrupted by noise. Here, we consider the best linear unbiased predictor for two cases, according to whether there is noise at the target untried location or not. We show that the mean squared prediction error does not converge to zero in either case. We investigate the use of stochastic Kriging in the prediction of Gaussian processes with input location error, and show that stochastic Kriging is a good approximation when the sample size is large. Several numeric examples are given to illustrate the results, and a case study on the assembly of composite parts is presented. Technical proofs are provided in the Appendix.

keywords: Gaussian process; Input location error; Stochastic Kriging; Composite parts assembly.

1 Introduction

Gaussian process modeling is widely used to recover underlying functions from scattered evaluations, possibly corrupted by noise. This method has been utilized in spatial statistics for several decades Matheron (1963); Cressie (2015). Later, Gaussian process modeling has been applied in computer experiments to build emulators of their outputs Sacks et al. (1989). In order to capture the randomness of real systems, it is natural to use stochastic simulation in computer experiments. For Gaussian process modeling, the output associated with each input can be decomposed as the sum of a mean Gaussian process output and random (Gaussian) noise. Following the terminology in design of experiments Wu and Hamada (2009), we call the noise added to the mean Gaussian process output as *extrinsic* noise. The extrinsic noise is usually from uncertainty associated with responses, such as measurement errors, computational errors and other unquantified errors. The corresponding Gaussian process modeling with extrinsic noise is called *stochastic Kriging* Ankenman et al. (2010). In spatial statistics, the noise is known as a nugget effect Matheron (1963).

¹ Wang and Wu's work is supported by NSF grant DMS 1564438. Wu's work is also supported by NSF grant DMS 1914632.

² Haaland's work is supported by NSF DMS 1621722 and DMS 1739097.

Besides extrinsic noise, in some cases, the input measurements are also corrupted by noise. Noisy or uncertain inputs are quite common in spatial statistics, because geostatistical data are often indexed by imprecise locations. Detailed examples can be found in Barber et al. (2006) and Veneziano and Van Dyck (1987). We call the input noise *intrinsic* noise. If the input measurements are corrupted by noise in a Gaussian process, it is known as a Gaussian process with input location error, and the corresponding best linear unbiased predictor is called Kriging adjusted for location error (KALE) Cressie and Kornak (2003). Also see Girard (2004); Dallaire et al. (2009); Bócsi and Csató (2013); McHutchon and Rasmussen (2011) for more discussions. KALE has been applied in a spectrum of arenas, including robotics Deisenroth et al. (2015), wireless networks Muppirisetty et al. (2016), and Wi-Fi fingerprinting He et al. (2017).

KALE predicts the mean Gaussian process output at an untried point *without* intrinsic noise. In some cases, however, the prediction of the mean Gaussian process output at an untried point *with* intrinsic noise is desired. A motivating example is the composite aircraft fuselage assembly process. In this process, a model is needed to predict the dimensional deviations under noisy actuators' forces. Further, when new actuator forces are implemented in practice, there is an inevitable intrinsic noise, i.e., uncertainty in the actually delivered actuator forces. Therefore, the output at an untried point has intrinsic noise. Under this scenario, we consider Kriging adjusting for location error and noise (KALEN), which is the best linear unbiased predictor of the mean Gaussian process output at an untried point with intrinsic noise.

In this paper, we discuss three predictors, KALE, KALEN, and stochastic Kriging, applied in prediction and uncertainty quantification of Gaussian process regression with input location error. We show that unlike Gaussian process regression without location error, the mean squared prediction error (MSPE) of these three predictors does not converge to zero as the sample size goes to infinity. Furthermore, we show that the limiting MSPE of KALEN and stochastic Kriging are equal if an untried point has intrinsic noise. We obtain an asymptotic upper bound on the MSPE of KALE and stochastic Kriging if there is no noise at an untried point. Numeric results indicate that if the sample size is relatively small and noise is relatively large, KALE or KALEN have a much smaller MSPE, and thus are desirable, compared with stochastic Kriging. We also compare the performance of KALEN and stochastic Kriging in the modeling of a composite parts assembly process problem. We find that the KALEN and stochastic Kriging are comparable across a range of small intrinsic noise levels, corresponding to a range of actuator tolerances, which is consistent with the theoretical analysis.

The remainder of this article is structured as follows. In Section 2, we formally state the problem, introduce KALE and KALEN, and show some asymptotic properties of the MSPE of KALE and KALEN. Section 3 presents some theoretical results when using stochastic Kriging in the prediction of Gaussian processes with input location error. Parameter estimation methods are discussed in Section 4, and numeric results are presented in Section 5. A case study of the composite parts assembly process is considered in Section 6. Technical proofs are given in the Appendix.

2 Gaussian Processes with Input Location Error

In this section, we introduce two predictors of the Gaussian processes with input location error, KALE and KALEN. We also give several asymptotic properties of KALE and KALEN.

2.1 Two Predictors of Gaussian Processes with Input Location Error

Suppose f is an underlying function defined on \mathbb{R}^d , and the values of f on a convex and compact set Ω are of interest. A standard tool to build emulators is Gaussian process regression (see Fang et al. (2005) and Santner et al. (2013), for example). Specifically, suppose $f \sim \text{GP}(m(\cdot), \sigma^2\Psi(\cdot, \cdot))$, where $m(\cdot)$ is the mean function, σ^2 is the variance, and Ψ is the correlation function. For the ease of mathematical treatment, we assume $m(\cdot) = 0$, which is equivalent to removing the mean surface and will not impact the following analysis. Suppose we observe the responses $f(x_1), \dots, f(x_n)$ on $X = \{x_1, \dots, x_n\} \subset \Omega$. Following the terminology in design of experiments Wu and Hamada (2009), we call $X = \{x_1, \dots, x_n\}$ design points.

For a Gaussian process with input location error, the input measurements are corrupted by noise. In this paper, we mainly focus on the intrinsic error and assume the responses are not influenced by the extrinsic error. Specifically, suppose the responses are perturbed by the intrinsic error, that is, we observe $y(x_j) = f(x_j + \epsilon_j)$ for $x_j \in X$, where the ϵ_j 's are i.i.d. random variables with mean 0, finite variance σ_ϵ^2 , and have a probability density function $h(\cdot)$.

Following the approach in Cressie and Kornak (2003), the best linear unbiased predictor of $f(x)$ on an untried point x is given by

$$p(Y; x) = \alpha_1^T Y + \alpha_2, \quad (1)$$

where $\alpha_1 \in \mathbb{R}^n, \alpha_2 \in \mathbb{R}$ are the solution to the optimization problem

$$\min_{(\alpha_1, \alpha_2)} \mathbb{E}(f(x) - p(Y; x))^2 = \min_{(\alpha_1, \alpha_2)} \mathbb{E}(f(x) - \alpha_1^T Y - \alpha_2)^2, \quad (2)$$

and the responses on the design points are $Y = (y(x_1), \dots, y(x_n))^T$. Note that

$$\begin{aligned} \mathbb{E}(f(x)y(x_j)) &= \sigma^2 \int \Psi(x, x_j + \epsilon_j) h(\epsilon_j) d\epsilon_j, \\ \mathbb{E}(y(x_j)y(x_k)) &= \begin{cases} \sigma^2 \Psi(x_j, x_j), & j = k, \\ \sigma^2 \iint \Psi(x_j + \epsilon_j, x_k + \epsilon_k) h(\epsilon_j) h(\epsilon_k) d\epsilon_j d\epsilon_k, & j \neq k. \end{cases} \end{aligned} \quad (3)$$

By plugging (3) in (2) and minimizing (2) with respect to (α_1, α_2) , we obtain the solution to (2) is $\alpha_1 = K^{-1}r(x)$ and $\alpha_2 = 0$, where $r(x) = (r(x, x_1), \dots, r(x, x_n))^T$ denotes the covariance vector between $f(x)$ and Y with

$$r(x, x_j) = \sigma^2 \int \Psi(x, x_j + \epsilon_j) h(\epsilon_j) d\epsilon_j, \quad (4)$$

and $K = (K_{jk})_{jk}$ denotes the covariance matrix with

$$K_{jk} = \begin{cases} \sigma^2 \Psi(x_j, x_j), & j = k, \\ \sigma^2 \iint \Psi(x_j + \epsilon_j, x_k + \epsilon_k) h(\epsilon_j) h(\epsilon_k) d\epsilon_j d\epsilon_k, & j \neq k. \end{cases} \quad (5)$$

Plugging $\alpha_1 = K^{-1}r(x)$ and $\alpha_2 = 0$ into (1), we find the best linear unbiased predictor of $f(x)$ is

$$\hat{f}(x) = r(x)^T K^{-1}Y. \quad (6)$$

Cressie and Kornak (2003) refer to (6) as Kriging adjusting for location error (KALE). If the prediction of $y(x)$ on an untried point x with intrinsic noise is of interest, it can be shown that we only need to replace $r(x)$ in (6) by $r_N(x) = (r_N(x, x_1), \dots, r_N(x, x_n))^T$, where

$$r_N(x, x_j) = \sigma^2 \iint \Psi(x + \epsilon, x_j + \epsilon_j) h(\epsilon_j) h(\epsilon) d\epsilon_j d\epsilon. \quad (7)$$

We refer to the corresponding best linear unbiased predictor $\hat{y}(x) = r_N(x)K^{-1}Y$ as Kriging adjusting for location error and noise (KALEN). One simple relation between KALE and KALEN is $\hat{y}(x) = \int \hat{f}(x + \epsilon)h(\epsilon)d\epsilon$.

In some cases, there exist closed forms of the integrals in (4)–(7). For example, if the correlation function $\Psi(s, t) = \exp(-\theta\|s - t\|_2^2)$, and the noise $\epsilon \sim N(0, \sigma_\epsilon^2 I_d)$, where $\theta > 0$ is the correlation parameter, and $N(0, \sigma_\epsilon^2 I_d)$ is a mean zero normal distribution with covariance matrix $\sigma_\epsilon^2 I_d$, then (4)–(7) can be calculated respectively as

$$\begin{aligned} K_{jk} &= \begin{cases} \sigma^2 & j = k, \\ \frac{\sigma^2}{(1+4\sigma_\epsilon^2\theta)^{d/2}} e^{-\frac{\theta\|x_j - x_k\|_2^2}{1+4\sigma_\epsilon^2\theta}} & j \neq k, \end{cases} \\ r(x, x_j) &= \frac{\sigma^2}{(1 + 2\sigma_\epsilon^2\theta)^{d/2}} e^{-\frac{\theta\|x - x_j\|_2^2}{1+2\sigma_\epsilon^2\theta}}, \\ r_N(x, x_j) &= \frac{\sigma^2}{(1 + 4\sigma_\epsilon^2\theta)^{d/2}} e^{-\frac{\theta\|x - x_j\|_2^2}{1+4\sigma_\epsilon^2\theta}}. \end{aligned} \quad (8)$$

Unfortunately, in general, equations (4)–(7) are intractable and need to be calculated via Monte Carlo integration by sampling ϵ from $h(\cdot)$, which can be computationally expensive. For example, if we choose the Matérn correlation function, then (6) does not have a closed form. In this case, the calculation of (6) will require much time, as we will see in Section 5.

2.2 The Mean Squared Prediction Error of KALE and KALEN

Now we consider the mean squared prediction error (MSPE) of KALE and KALEN. The MSPE of KALE can be calculated by

$$\begin{aligned} \mathbb{E}(f(x) - \hat{f}(x))^2 &= \mathbb{E}(f(x) - r(x)^T K^{-1}Y)^2 \\ &= \mathbb{E}(f(x)^2) - 2r(x)^T K^{-1}\mathbb{E}(f(x)Y) + r(x)^T K^{-1}\mathbb{E}(YY^T)K^{-1}r(x) \\ &= \sigma^2 \Psi(x, x) - r(x)^T K^{-1}r(x), \end{aligned} \quad (9)$$

where \hat{f} is as in (6), and r and K are as defined in (4) and (5), respectively. The last equality is true because of (3). Similarly, one can check the MSPE of KALEN is

$$\mathbb{E}(y(x) - \hat{y}(x))^2 = \sigma^2 \Psi(x, x) - r_N(x)^T K^{-1} r_N(x), \quad (10)$$

where r_N is as defined in (7).

Define

$$\Psi_S(s, t) = \iint \Psi(s + \epsilon_1, t + \epsilon_2) h(\epsilon_1) h(\epsilon_2) d\epsilon_s d\epsilon_t. \quad (11)$$

In Proposition 3.1 of Cervone and Pillai (2015), it is shown that if a function $c(s, t) = \Psi_S(s, t)$ for $s \neq t$ and $c(s, s) = \Psi(s, s)$, then $c(\cdot, \cdot)$ is a valid correlation function. Therefore, the covariance matrix K defined in (5) is positive definite. We first consider the asymptotic properties of (10) as the fill distance goes to zero, where the fill distance h_X of the design points X is defined by

$$h_X := \sup_{x \in \Omega} \min_{x_j \in X} \|x - x_j\|_2. \quad (12)$$

Notice that the MSPE of KALEN can be expressed as

$$\begin{aligned} E(y(x) - \hat{y}(x))^2 &= \sigma^2 \Psi(x, x) - r_N(x)^T K^{-1} r_N(x) \\ &= \sigma^2 (\Psi(x, x) - \Psi_S(x, x)) + \sigma^2 \Psi_S(x, x) - r_N(x)^T K^{-1} r_N(x). \end{aligned} \quad (13)$$

Let $K_S = \sigma^2 (\Psi_S(x_j, x_k))_{jk}$. Thus, $K = K_S + \sigma^2 (\Psi(x, x) - \Psi_S(x, x)) I_n$. In the rest of Section 2 and Section 3, we assume the correlation function $\Psi(\cdot, \cdot)$ satisfies the following assumption.

Assumption 1. Ψ is a radial basis function, i.e., $\Psi(s, t) = \phi(\|s - t\|_2)$ for $s, t \in \Omega$. Furthermore, assume Ψ has continuous second order derivatives and $\phi(r) > 0$ is a decreasing function of $r \in \mathbb{R}^+$, with $\phi(0) = 1$.

Many widely used correlation functions, including isotropic Gaussian correlation functions and isotropic Matérn correlation functions, satisfy this assumption. For anisotropic correlation functions that have form $\Psi(s, t) = \phi(\|A(s - t)\|_2)$ with A an diagonal positive definite matrix and $s, t \in \Omega$, we can stretch the space Ω to Ω' such that $\Psi(s', t') = \phi(\|s' - t'\|_2)$ for $s', t' \in \Omega'$ is satisfied. Assumption 1 implies $\Psi_S(x, x) \leq \Psi(x, x)$. Intuitively K is equal to a covariance matrix plus a nugget parameter. In order to justify this intuition, we need to show that K_S is a covariance matrix, which follows from the fact that $\Psi_S(\cdot, \cdot)$ is a positive definite function, as stated in the following lemma whose proof is given in Appendix B.

Lemma 1. *If $\Psi(\cdot, \cdot)$ is a positive definite function, then $\Psi_S(\cdot, \cdot)$ is a positive definite function.*

In order to study the asymptotic performance of KALE and KALEN, we consider a sequence of designs X_m . We assume the following.

Assumption 2. *The sequence of design points X_m satisfies that there exists a constant $C > 0$ such that $h_{X_m} \leq C q_{X_m}$ for all m , where*

$$q_X = \min_{1 \leq j \neq k \leq n} \|x_j - x_k\|/2$$

for $X = \{x_1, \dots, x_n\}$, and $\text{card}(X_m) = n_m$.

It is not hard to find designs satisfy this assumption. For example, grid designs satisfy Assumption 2. In the rest of paper we suppress the dependence of X on m for notational simplicity. It can be shown that if a Gaussian process has no intrinsic noise, then the MSPE of the corresponding best linear unbiased predictor converges to zero as the fill distance goes to zero. Unlike a Gaussian process without input location error, we show that the limit of the MSPE of KALE and KALEN are usually not zero. In fact, (13) and Lemma 1 imply that the MSPE of KALEN is the MSPE of a Gaussian process with extrinsic error plus a non-zero constant. These results are stated in Theorem 1, whose proof is provided in Appendix C.

Theorem 1. *The MSPE of KALEN (10) converges to $\sigma^2(\Psi(x, x) - \Psi_S(x, x))$ as the fill distance of the design points converges to zero, where Ψ_S is defined in (11).*

In Theorem 1, we present a limit of the MSPE of KALEN. The limit $\sigma^2(\Psi(x, x) - \Psi_S(x, x))$ is usually not zero. This is expected for KALEN since there is a random error at the untried point x . The MSPE limit depends on two parts. One is the variance σ^2 and the other is the difference $\Psi(x, x) - \Psi_S(x, x)$. The variance σ^2 depends on the underlying process, while the difference depends on the distribution of the noise h . Roughly speaking, the difference $\Psi(x, x) - \Psi_S(x, x)$ will be larger if the density h is more spread out.

One might expect that the MSPE of KALE converges to zero as the fill distance of the design points goes to zero. However, the following proposition shows that, in the case of Gaussian correlation functions and normally distributed intrinsic error, there is a positive lower bound on the MSPE of KALE. The proof can be found in Appendix D.

Proposition 1. *Suppose the covariance function $\Psi(s, t) = \exp(-\theta\|s - t\|_2^2)$ for some $\theta > 0$, and the input noise $\epsilon_j \sim N(0, \sigma_\epsilon^2)$ are i.i.d., where $N(0, \sigma_\epsilon^2)$ is a mean zero normal distribution with variance σ_ϵ^2 . Then for any design $X = \{x_1, \dots, x_n\} \subset \Omega$, the MSPE of KALE, defined in (9), has a lower bound*

$$\sigma^2 \left(1 - \frac{(1 + 4\sigma_\epsilon^2\theta)^{d/2}}{(1 + 2\sigma_\epsilon^2\theta)^d} \right).$$

From Theorem 1 and Proposition 1, we can see that unlike Gaussian processes with only extrinsic error, the MSPEs of the predictors for Gaussian processes with input location error do not converge to zero, unless $\sigma_\epsilon^2 = 0$.

3 Comparison Between KALE/KALEN and Stochastic Kriging

It is argued in Cressie and Kornak (2003) and Stein (1999) that using a nugget parameter is one way to counteract the influence of noise within the inputs. Therefore, it is natural to ask whether stochastic Kriging is a good approximation method to predict the value at an untried point, since it is not the best linear unbiased predictor under the settings of Gaussian process with input location error. Cervone and Pillai (2015) claim that a nugget parameter alone cannot capture the effect of input location error. In this paper, we show that the MSPE of stochastic Kriging has the same limit as the MSPE of KALEN, and provide an upper bound on the MSPE of stochastic Kriging if the untried point has no noise, as stated in the following theorem. The proof can be found in Appendix E.

Theorem 2. Let $\mu > 0$ be a constant, where $\Psi_S(\cdot, \cdot)$ is as defined in (11). A stochastic Kriging predictor of Gaussian process with input location error is defined as

$$\hat{f}_S(x) = \Psi(x, X)(\Psi(X, X) + \mu I_n)^{-1}Y, \quad (14)$$

where $\Psi(x, X) = (\Psi(x, x_1), \dots, \Psi(x, x_n))^T$ and $\Psi(X, X) = (\Psi(x_j, x_k))_{jk}$.

(i) Suppose there is noise at an untried point. The MSPE of the predictor (14) has the same limit as KALEN, which is $\sigma^2(\Psi(x, x) - \Psi_S(x, x))$, when the fill distance of X goes to zero, where Ψ_S is defined in (11).

(ii) Suppose there is no noise at an untried point. An asymptotic upper bound on the MSPE of the predictor (14) is

$$\frac{2\sigma^2}{(2\pi)^d} \int_{\mathbb{R}^d} |1 - |b(t)||^2 |\mathcal{F}(\Psi)(t)| dt, \quad (15)$$

where $\mathcal{F}(\Psi)$ is the Fourier transform of Ψ and $b(t) = \mathbb{E}(e^{ic^T t})$ is the characteristic function of h .

Remark 1. We say b is an asymptotic upper bound on a sequence a_n , if there exists a sequence b_n such that $a_n \leq b_n$ and $\lim_{n \rightarrow \infty} b_n = b$.

Theorem 2 shows that the predictor (14) is as good as KALEN asymptotically. The following proposition states that if the noise is small, then (15) can be controlled. The proof of Proposition 2 can be found in Appendix F.

Proposition 2. Suppose $\{\epsilon_n\}$ is a sequence of random variables that converges to 0 in distribution. Let

$$a_n = \frac{\sigma^2}{(2\pi)^d} \int_{\mathbb{R}^d} |1 - |b_n(t)||^2 |\mathcal{F}(\Psi)(t)| dt, \quad (16)$$

where $b_n(t) = \mathbb{E}(e^{i\epsilon_n^T t})$. Then a_n converges to zero.

One advantage of stochastic Kriging is that we can simplify the calculation since we do not need to calculate the integrals in (5) and (7). If the noise is small and the fill distance is small, Theorem 2 and Proposition 2 state that the MSPE of the predictor (14) can be comparable with the best linear unbiased predictor.

As we mentioned before, it is argued in Cervone and Pillai (2015) that since the integrated covariance function in (5) is not the same as the covariance function in the original Gaussian process without location error, a nugget parameter alone cannot capture the effect of location error. It is true that the MSPE of KALE or KALEN is the smallest among all the linear unbiased predictors. However, our results also show that with an appropriate nugget parameter, the predictor (14) is as good as KALEN asymptotically, and there is little difference between KALE and the predictor (14) if the variance of the intrinsic noise and the fill distance are small.

For the ease of mathematical treatment, we assume the noise ϵ_i 's are i.i.d. If ϵ_i 's are independent but not identical, the proof is similar. As a special case, if the underlying process has a Gaussian correlation function, and the intrinsic noise is normally distributed,

the lower bound of KALE and the asymptotic upper bound of the predictor (14) can be calculated analytically. We have the following corollary, which is a direct result of Theorem 2, and the proof is omitted.

Corollary 1. *Suppose the covariance function and the intrinsic noise are as in Proposition 1. If there is noise at an untried point x , the stochastic Kriging predictor has the same asymptotic MSPE of KALEN, which is $\sigma^2 \left(1 - \frac{1}{(1+4\sigma_\epsilon^2\theta)^{d/2}}\right)$. If there is no noise at an untried point x , the asymptotic upper bound of MSPE for stochastic Kriging is*

$$\frac{2\sigma^2}{(2\pi)^d} \int_{\mathbb{R}^d} |1 - |b(t)||^2 |\mathcal{F}(\Psi)(t)| dt = 2\sigma^2 \left(1 + \frac{1}{(1 + 4\sigma_\epsilon^2\theta)^{d/2}} - \frac{2}{(1 + 2\sigma_\epsilon^2\theta)^{d/2}}\right).$$

Note that KALE is the best linear unbiased predictor for the prediction of output at an untried point without noise. Therefore, the upper bound of MSPE for stochastic Kriging is also an upper bound of KALE. Corollary 1 implies that the asymptotic MSPE of KALE is smaller than the MSPE of KALEN, which is true intuitively. The MSPE of KALE/KALEN is close to zero if the variance of noise σ_ϵ^2 is small. Corollary 1 also implies that the MSPE of KALE/KALEN increases as the input dimension increases.

4 Parameter Estimation

An accuracy preserving and computationally feasible technique for estimating the unknown parameters is necessary to actually apply the noisy input model described above. An intuitive approach to estimate the parameters is maximum likelihood estimation. Up to a multiplicative constant, the likelihood function is

$$\ell(\theta; X, Y) \propto \int \dots \int |\Sigma_1|^{-1/2} e^{-\frac{1}{2}y^T \Sigma_1^{-1}y} h(\epsilon_1) \dots h(\epsilon_n) d\epsilon_1 \dots d\epsilon_n, \quad (17)$$

where $\Sigma_1 = (\sigma^2 \Psi(x_j + \epsilon_j, x_k + \epsilon_k))_{jk}$. Unfortunately, the integral in (17) is difficult to calculate, because the dimension of the integral increases as the sample size increases. In this work, we use a pseudo-likelihood approach proposed by Cressie and Kornak (2003). Define

$$\ell_g(\theta; X, Y) = (2\pi)^{-n/2} |K|^{-1/2} \exp\left(-\frac{1}{2}Y^T K^{-1}Y\right), \quad (18)$$

where θ are parameters we want to estimate, and K is defined in (5). The maximum pseudo-likelihood estimator can be defined as

$$\hat{\theta}_1 = \arg \sup_{\theta} \ell_g(\theta). \quad (19)$$

Because of non-identifiability, parameters inside the Gaussian process and σ_ϵ cannot be estimated simultaneously Cervone and Pillai (2015). The properties of the pseudo-likelihood approach are discussed in Cervone and Pillai (2015). Here we list a few of them. First, the pseudo-score provides an unbiased estimation equation, i.e.,

$$\mathbb{E}(S(\theta; Y)) = \mathbb{E}(\nabla \log(\ell_g(\theta; X, Y))) = 0.$$

Second, the covariance matrix of the pseudo-score $\mathbb{E}(S(\theta; Y)S(\theta; Y)^T)$ and the expected negative Hessian of the log pseudo likelihood $\mathbb{E}\left(\frac{\partial^2}{\partial\theta_j\partial\theta_k}\log(\ell_g(\theta; X, Y))\right)$ can be calculated. However, the consistency of parameters estimated by pseudo-likelihood in the case of Gaussian process has not been theoretically justified to the best of our knowledge.

If we use stochastic Kriging, the corresponding (misspecified) log likelihood function is, up to an additive constant,

$$\ell_{nug}(\theta, \mu; X, Y) = -\frac{1}{2}\log(|\Psi(X, X) + \mu I_n|) - \frac{1}{2}Y^T(\Psi(X, X) + \mu I_n)^{-1}Y, \quad (20)$$

The maximum likelihood estimator of (θ, μ) is defined by

$$(\hat{\theta}_2, \hat{\mu}) = \arg \sup_{\theta} \ell_{nug}(\theta, \mu; X, Y). \quad (21)$$

Note that the log likelihood function (20) is the log likelihood function for a Gaussian process with only extrinsic noise. Thus it is misspecified, and the estimated parameters may also be misspecified. However, it has been shown by Ying (1991) and Zhang (2004) that the Gaussian process model parameters in the covariance functions may not have consistent estimators. Therefore, using Gaussian process models for prediction may be more meaningful than for parameter estimation. In fact, the parameter estimates do not significantly influence our theoretical results on the MSPE of KALE, KALEN and stochastic Kriging, in the sense of the following theorem.

Theorem 3. *Suppose for some constant $C > 0$, $1/C \leq \hat{\mu} \leq C$ for all n . Let $\hat{\Psi}_1$ and $\hat{\Psi}_2$ be the correlation functions with estimated parameters $\hat{\theta}_1$ and $\hat{\theta}_2$ as in (19) and (21), respectively. Potential dependency of $\hat{\mu}$, $\hat{\Psi}_1$ and $\hat{\Psi}_2$ on n is suppressed for notational simplicity. Assume the following.*

(1) *There exists a constant A_1 such that for all n*

$$\max \left\{ \left\| \frac{\mathcal{F}(\Psi)}{\mathcal{F}(\hat{\Psi}_1)} \right\|_{L_\infty}, \left\| \frac{\mathcal{F}(\Psi)}{\mathcal{F}(\hat{\Psi}_2)} \right\|_{L_\infty} \right\} \leq A_1. \quad (22)$$

(2) *Assumption 1 is true for all n . Furthermore, assume the second order derivatives of $\hat{\Psi}_1$ and $\hat{\Psi}_2$ have a uniform upper bound for all n .*

(3) *Assumption 2 is true for designs X .*

Then the following statements are true.

(i) *Suppose there is noise at an untried point x . Then the MSPEs of KALEN and stochastic Kriging have the limit $\sigma^2(\Psi(x, x) - \Psi_S(x, x))$ when the fill distance of X goes to zero, where Ψ_S is defined in (11).*

(ii) *Suppose there is no noise at an untried point x . An asymptotic upper bound on the MSPE of KALE and stochastic Kriging is*

$$\frac{2\sigma^2}{(2\pi)^d} \int_{\mathbb{R}^d} |1 - |b(t)|^2| \mathcal{F}(\Psi)(t) dt,$$

where $b(t) = \mathbb{E}(e^{ic^T t})$ is the characteristic function of h .

Theorem 3 states that if the pseudo-likelihood ℓ_g and the mis-specified likelihood ℓ_{nug} can provide reasonable estimated parameters, then we have the following: (1) If an untried point has noise, the limit of the MSPE of KALEN and stochastic Kriging remains the same; and (2) If an untried point has no noise, the upper bounds on the MSPE of KALE and stochastic Kriging can be obtained. The limit and upper bounds are small if the noise is small. These upper bounds are the same as the bounds in Theorem 2. Therefore, the parameter estimation does not significantly influence our theoretical analysis.

The computation complexity of (21) is about the same as that of (19), if (5) can be calculated analytically. Unfortunately, (5) usually does not have a closed form, which substantially increases the computation time of solving (19).

5 Numeric Results

In this section, we report some simulation studies to investigate the numeric performance of KALE, KALEN and stochastic Kriging. In Example 1, we use Gaussian correlation functions to fit a 1-d function, where the predictor (6) has analytic form. In Example 2, we use Matérn correlation functions to fit a 2-d function, where the integrals in (4) and (5) need to be calculated by Monte-Carlo Cressie and Kornak (2003).

In both examples, we also include comparisons to a Markov chain Monte Carlo (MCMC) method along the lines described in Cervone and Pillai (2015). The MCMC methods provide an alternative way to predict Gaussian process regression with input location error as well as parameter estimation. Recall that $f(x)$ and $y(x)$ are responses on an untried point x with and without intrinsic error, respectively. The MSPE-optimal predictors of $f(x)$ and $y(x)$ are given by

$$\begin{aligned}\hat{f}_B(x) &= \int r_B(x, X + \epsilon_B) \Psi(X + \epsilon_B, X + \epsilon_B)^{-1} Y \pi(\theta, \epsilon_B | Y) d\epsilon_B d\theta, \\ \hat{y}_B(x) &= \int r_B(x + \epsilon, X + \epsilon_B) \Psi(X + \epsilon_B, X + \epsilon_B)^{-1} Y \pi(\theta, \epsilon_B | Y) d\epsilon_B d\theta,\end{aligned}\quad (23)$$

respectively, where $\epsilon_B = (\epsilon_1, \dots, \epsilon_n)^T$ is the noise vector, $r_B(s, X + \epsilon_B) = (\Psi(s, x_1 + \epsilon_1), \dots, \Psi(s, x_n + \epsilon_n))$ for $s = x$ or $x + \epsilon$, $\Psi(X + \epsilon_B, X + \epsilon_B) = (\Psi(x_j + \epsilon_j, x_k + \epsilon_k))_{jk}$, θ are parameters, and $\pi(\theta, \epsilon_B | Y)$ is the conditional distribution of θ, ϵ_B given Y . The conditional distribution $\pi(\theta, \epsilon_B | Y)$ does not have a closed form, and needs to be calculated by MCMC. By Bayes rule, $\pi(\theta, \epsilon_B | Y) \propto \pi(Y | \theta, \epsilon_B) \pi(\epsilon_B | \theta) \pi(\theta)$. The conditional distribution $\pi(Y | \theta, \epsilon_B)$ is normal, and $\pi(\epsilon_B | \theta)$ is the conditional distribution of noise, given parameter θ . In practice, it is often assumed that $\pi(\epsilon_B | \theta)$ is another normal distribution, and $\pi(\theta)$ is a uniform distribution over a region Cervone and Pillai (2015).

5.1 Example 1

Suppose the underlying function is $f(x) = \sin(2\pi x/10) + 0.2 \sin(2\pi x/2.5)$, $x \in [0, 8]$ Higdon (2002). The design points are selected to be 161 evenly spaced points on $[0, 8]$. The intrinsic noise is chosen to be mean zero normal distributed with the variances $0.05k$, for $k = 1, 2, 3, 4$. We use a Gaussian correlation function $\Psi(s, t) = \sigma^2 \exp(-\theta \|s - t\|_2^2)$ to make predictions,

and use the pseudo likelihood approach presented in Section 4 to estimate the unknown parameters. For each variance of intrinsic noise, we approximate the squared L_2 error $\|f - \hat{f}\|_2^2$ by $\frac{8}{n} \sum_{i=1}^n (f(x_i) - \hat{f}(x_i))^2$, where the x_i 's are 8001 evenly spaced points on $[0, 8]$. Then we run 100 simulations and take the average of $\frac{8}{n} \sum_{i=1}^n (f(x_i) - \hat{f}(x_i))^2$ to estimate $\mathbb{E}\|f - \hat{f}\|_2^2$. We estimate $\mathbb{E}\|y - \hat{y}\|_2^2$ by a similar approach. Recall that $\mathbb{E}\|f - \hat{f}\|_2^2$ and $\mathbb{E}\|y - \hat{y}\|_2^2$ are related to KALE and KALEN, respectively. With an abuse of terminology, we still call $\mathbb{E}\|f - \hat{f}\|_2^2$ and $\mathbb{E}\|y - \hat{y}\|_2^2$ MSPE.

In order to make a comprehensive comparison, we also include the results from the Markov chain Monte Carlo method. After 1000 burn-in runs, we run 40 iterations for prediction, i.e., calculating $\hat{f}_B(x)$ and $\hat{y}_B(x)$ in (23). The prior we choose is $\theta \sim \text{Unif}[0.1, 0.2]$, $\sigma \sim \text{Unif}[0, 5]$, and $\sigma_\epsilon \sim \text{Unif}[0.01, 0.02]$. The final results are not sensitive to the choices of priors.

The RMSPE results, which is the square root of MSPE, for KALE/KALEN, stochastic Kriging, and MCMC, are shown in Table 1/Table 2, respectively.

σ_ϵ^2	RMSPE of KALE	RMSPE of stochastic Kriging	Difference	RMSPE of MCMC
0.05	0.1020	0.1114	0.0093	0.2448
0.10	0.1718	0.1836	0.0118	0.2105
0.15	0.2161	0.2379	0.0218	0.2434
0.20	0.2530	0.3000	0.0470	0.2702

Table 1: Comparison of the RMSPE for KALE, stochastic Kriging, and MCMC: 1-d function with Gaussian correlation function. In fourth column, difference = 3rd column – 2nd column, i.e., the RMSPE of stochastic Kriging – the RMSPE of KALE.

σ_ϵ^2	RMSPE of KALEN	RMSPE of stochastic Kriging	Difference	RMSPE of MCMC
0.05	0.2526	0.2522	-0.0004	0.5847
0.10	0.2820	0.2827	0.0007	0.5872
0.15	0.3138	0.3212	0.0074	0.5905
0.20	0.3624	0.3841	0.0217	0.5876

Table 2: Comparison of the RMSPE for KALEN, stochastic Kriging, and MCMC: 1-d function with Gaussian correlation function. In fourth column, difference = 3rd column – 2nd column, i.e., the RMSPE of stochastic Kriging – the RMSPE of KALEN.

It can be seen from Tables 1 and 2 that the RMSPE of KALE/KALEN and stochastic Kriging decreases as the variance of the intrinsic noise decreases. This corroborates the results in Theorem 2 and Proposition 2. The difference of RMSPE between KALE/KALEN and stochastic Kriging also decreases when the variance of the intrinsic noise decreases. Comparing Table 2 with Table 1, it can be seen that the RMSPE of KALEN is larger than that of KALE. This is reasonable because KALEN predicts $y(x)$, which includes an error term while $f(x)$ does not. The computation of KALE/KALEN has the same complexity as the stochastic Kriging in this example, because a Gaussian correlation function is used, and

the integrals in (5) and (7) can be calculated analytically. In all cases, the RMSPE of the direct MCMC approach is larger than KALE/KALEN and stochastic Kriging.

In order to further understand the performance of KALE and stochastic Kriging, one realization among the 100 simulations for Table 1 is illustrated in Figure 1, where the variance of the intrinsic noise is chosen to be 0.05. In Figure 1, the circles are the collected data points. The true function, the prediction curves of KALE and stochastic Kriging are denoted by solid line, dashed line and dotted line, respectively. It can be seen from the figure that both KALE and stochastic Kriging approximate the true function well.

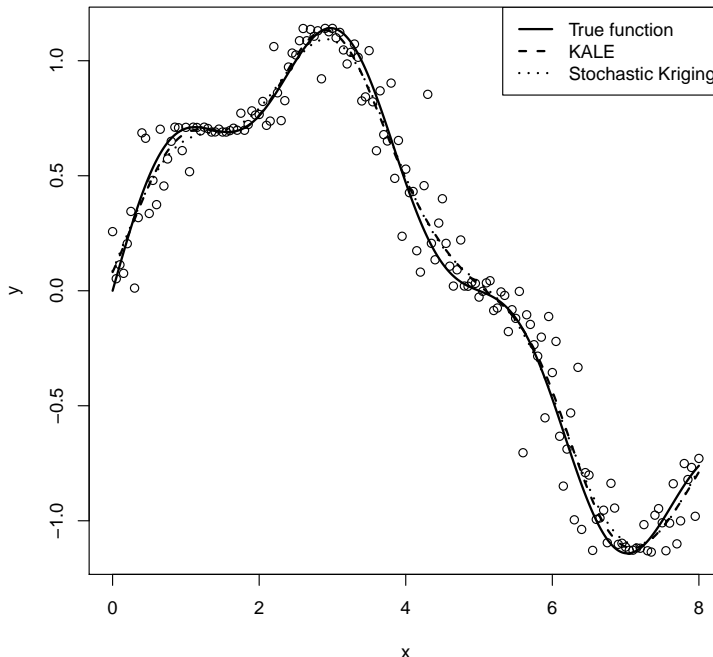


Figure 1: An illustration of KALE and stochastic Kriging.

5.2 Example 2

In this example, we compare the calculation time of stochastic Kriging and KALE, where the predictor (6) of KALE does not have an analytic form. Suppose the underlying function is $f(x) = [(30 + 5x_1 \sin(5x_1))(4 + \exp(-5x_2)) - 100]/6$ for $x_1, x_2 \in [0, 1]$ Lim et al. (2002). We use the Matérn correlation functions Stein (1999)

$$\Phi(x; \nu, \phi) = \frac{1}{\Gamma(\nu)2^{\nu-1}} (2\sqrt{\nu}\phi\|x\|_2)^\nu K_\nu(2\sqrt{\nu}\phi\|x\|_2), \quad (24)$$

to make predictions, where K_ν is the modified Bessel function of the second kind; and ν and ϕ are model parameters. The Matérn correlation function can control the smoothness of the predictor by ν and thus is more robust than a Gaussian correlation function Wang

et al. (2019). The covariance function is chosen to be $\Psi(x, y) = \sigma^2 \Phi(x - y; \nu, \phi)$. We use maximin Latin hypercube design with 20 points to estimate parameters, and choose the first 100 points in the Halton sequence Halton (1964) as test points. The smoothness parameter ν is chosen to be 3, which can provide a robust estimator of f .

If we use a Matérn correlation function, the integrals in (4) and (5) do not have analytic forms and are calculated by Monte-Carlo. We randomly choose 30 points to approximate the integral in (4), and 900 points to approximate the integral in (5). Preliminary results show that, if we use Monte-Carlo with different points every time in the evaluation of the integrals in (4) and (5), it is not possible to use maximum pseudo likelihood estimation to estimate the unknown parameters, consisting of ϕ in (24), σ^2 , the variance of noise σ_ϵ^2 and the mean β . The reason is that at each step of the optimization in maximum pseudo likelihood estimation, we need to calculate the integral, whose computational cost is high. Therefore, we generate 900 points and 30 points randomly one time and use these 900 points and 30 points for evaluations of (5) and (4), respectively. Then we use maximum pseudo likelihood to estimate the unknown parameters.

For stochastic Kriging, we use maximum likelihood to estimate the unknown parameters, which are ϕ in (24), σ^2 , the nugget parameter μ and the mean β . For MCMC, we use 1000 burn-in runs, and 40 runs for calculating the predictor. The prior we choose is $\theta \sim \text{Unif}[0.1, 0.2]$, $\sigma \sim \text{Unif}[4, 5]$, $\sigma_\epsilon \sim \text{Unif}[0.01, 0.02]$, $\beta \sim \text{Unif}[0, 4]$. The RMSPE and the processing time of KALE and stochastic Kriging are shown in Table 3.

σ_ϵ^2	RMSPE of KALE	PT of KALE	RMSPE of SK	PT of SK	Difference	RMSPE of MCMC	PT of MCMC
0.02	1.780	646.38	1.819	6.85	0.039	1.447	40.45
0.03	1.091	884.84	1.779	5.56	0.688	1.514	40.41
0.04	1.320	868.49	1.833	5.73	0.513	1.607	41.65
0.05	2.270	1134.98	2.382	5.25	0.112	1.758	37.03

Table 3: The RMSPE of KALE, stochastic Kriging, and MCMC: 2-d function with Matérn correlation function. The processing time is in seconds. In sixth column, difference = 4th column – 2nd column, i.e., the RMSPE of stochastic Kriging – the RMSPE of KALE. The following abbreviation is used: PT = Processing time, SK = stochastic Kriging

It can be seen that KALE has some improvement on prediction accuracy over stochastic Kriging. However, KALE takes too much computation time, even though the numbers of design points and test points are relatively small. The comparison would get worse as the number of points became larger. For MCMC, although it may improve the prediction, it is very sensitive to the initial choices of priors. The multimodality discussed in Cervone and Pillai (2015) could be a potential reason. The processing time for the MCMC approach is much larger than stochastic Kriging, but smaller than KALE. Since our main focus is on the comparison between KALE and stochastic Kriging, we do not further discuss the numeric results of MCMC. Therefore, if the integrals in (4) and (5) do not have analytic forms, stochastic Kriging is preferred, especially when the sample size is large and the variance of intrinsic noise is small.

6 Case Study: Application in Composite Parts Assembly Process

To illustrate the performance of KALEN and stochastic Kriging, we apply them to a real case study, the composite parts assembly process. As shown in Figure 2 (a) and Figure 2 (b), ten adjustable actuators are installed at the edge of a composite part Yue et al. (2018); Wen et al. (2018). These actuators can provide push or pull forces in order to adjust the shape of the composite part to the target dimensions. The dimensional shape adjustment of composite parts is one of the most important steps in the aircraft assembly process. It reduces the gap between the composite parts and decreases the assembly time with improved dimensional quality. Detailed descriptions about the shape adjustment of composite parts can be found in Wen et al. (2018). Modeling of composite parts is the key for shape adjustment. The objective is to build a model that has the capability to predict the dimensional deviations accurately under specific actuators' forces. In this model, the input variables are ten actuators' forces. The responses are the dimensional deviations of multiple critical points along the edge plane near the actuators, shown in Figure 2 (c). We consider responses at 91 critical points around the composite edge in the case study.

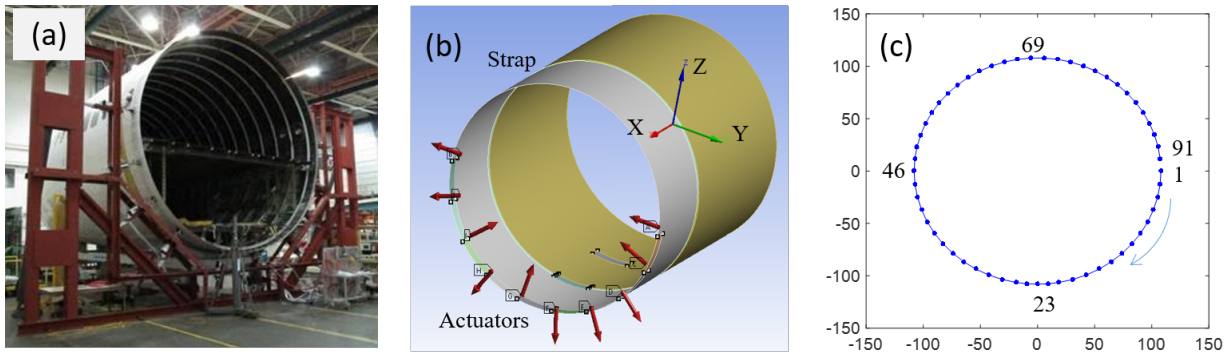


Figure 2: Schematic diagram for composite part shape adjustment: (a) composite part shape adjustment Wen et al. (2018), (b) layout of ten actuators, (c) multiple critical points.

In the shape control of composite parts, intrinsic noise commonly exists in the actuators' forces Yue et al. (2018). When a force is implemented by an actuator, the real force may not be exactly same as the target force. The magnitudes of forces may have uncertainties naturally due to the device tolerances of the hydraulic or electromechanical system of actuators. Uncertainties in the directions and application points of forces come from the deviations of contact geometry of actuators and their installations. For the modeling of composite parts, there are two steps: (i) training the parameters using experimental data; (ii) predicting dimensional deviations for new actuators' forces. In the training step, we need to consider input error in the experimental data. Additionally, when new actuator forces are implemented in practice, the uncertainty in the actual delivered forces inevitably exists. This suggests that KALEN is suitable for this application scenario. We will show the performance of KALEN and compare it with stochastic Kriging as follows.

The model we use in this case study is $Y^{(j)} = F^T \beta^{(j)} + Z^{(j)}(x)$ for $j = 1, \dots, 91$, where

$Y^{(j)}$ is the dimensional deviation vector of the composite part at the critical point j and $Z^{(j)}(\cdot)$ is a mean zero Gaussian random field, with variables in \mathbb{R}^{10} . The correlation function of $Z^{(j)}(\cdot)$ is assumed to be $\exp(-\sum_{k=1}^{10} \theta_{jk}(s_k - t_k)^2)$, where $\theta_{jk} > 0$ are parameters. The variance of $Z^{(j)}(\cdot)$ is denoted by σ_j^2 . The parameters $\beta^{(j)}$, θ_{jk} , σ_ϵ^2 , and σ_j^2 are estimated by maximum (pseudo-)likelihood estimation as described in Section 4. The mean function $F^T \beta^{(j)}$ we use in this model is to represent the linear component in dimensional shape control of composite fuselage, which follows the approach in Yue et al. (2018). Specifically, according to the mechanics of composite material and classical lamination theory, there is a linear relationship between dimensional deviations and actuators' forces within the elastic zone. The term $F^T \beta^{(j)}$ describes how the actuators' forces impact the part deviations linearly, and $Z^{(j)}(\cdot)$ represents the nonlinear components so as to get accurate predictions.

For the computer experiments, we generated 50 training samples and 30 testing samples based on a maximin Latin hypercube design. The designed experiments are conducted in the finite element simulation platform developed by Wen et al. (2018). It is worth mentioning that the computer simulation here is not a deterministic simulation. The intrinsic noise is added to the actuators' forces to mimic real actuators. The standard deviations (SD) of actuators' forces are chosen to be 0.005, 0.01, 0.02, 0.03, and 0.04 lbf (lbf is a unit of pound-force), which is determined by the tolerance of different kinds of actuators according to engineering domain knowledge. The maximum actuators' force is set to 600 lbf. After we have the computer experiment data, we can estimate the parameters of KALEN by solving the pseudo-likelihood equation (19), and the parameters of stochastic Kriging by solving the maximum likelihood equation (21). Then, we can use the model to predict dimensional deviations at the untried points in the testing dataset.

The performance of KALEN and stochastic Kriging are compared in terms of mean absolute error (MAE). This is an index that has been commonly used in the composite parts assembly domain to evaluate the modeling performance. We also compare RMSPE of KALEN and stochastic Kriging. The MAE and RMSPE are approximated by averaging the error on the 91 points and multiple samples.

SD of actuators' forces	MAE (RMSPE) of KALEN	MAE (RMSPE) of stochastic Kriging	Difference
0.005	0.0059 (0.0081)	0.0059 (0.0081)	7.1×10^{-7} (1.9×10^{-6})
0.01	0.0117 (0.0147)	0.0119 (0.0151)	1.7×10^{-4} (3.7×10^{-4})
0.02	0.0216 (0.0265)	0.0217 (0.0264)	9.5×10^{-5} (-8.7×10^{-5})
0.03	0.0286 (0.0335)	0.0304 (0.0376)	1.7×10^{-3} (4.1×10^{-3})
0.04	0.0389 (0.0478)	0.0486 (0.0610)	9.7×10^{-3} (1.3×10^{-2})

Table 4: The MAE (RMSPE) of KALEN and stochastic Kriging in the composite part modeling. In last column, difference = 3rd column - 2nd column.

The MAE and RMSPE of KALEN and stochastic Kriging are summarized in Table 4. As the SD of actuators' forces changes from 0.04 lbf to 0.005 lbf, the MAE and RMSPE of KALEN and stochastic Kriging also decrease. This result is consistent with the conclusions in Theorem 2 and Proposition 2. The MAE and RMSPE of KALEN are slightly smaller than the MAE and RMSPE of stochastic Kriging. Generally speaking, their performances

are comparable, especially when the SD of actuators' forces is small. The main reason is that, when the uncertainty in the input variables is small, stochastic Kriging can approximate the best linear unbiased predictor KALEN very well. Since a Gaussian correlation function is used, the computational complexity of KALEN and stochastic Kriging are the same. In summary, if high-quality actuators are used and the intrinsic noise in the actuators is therefore small, then both KALEN and stochastic Kriging can realize very good prediction performance. When the intrinsic noise in the actuators' forces becomes larger, KALEN outperforms stochastic Kriging.

7 Conclusions and Discussion

We first summarize our contributions in this work. We have investigated three predictors, KALE, KALEN and stochastic Kriging, as applied to Gaussian processes with input location error. When predicting the mean Gaussian process output at an untried point with intrinsic noise, we prove that the limits of MSPE of KALEN and stochastic Kriging are the same as the fill distance of the design points goes to zero. If there is no noise at an untried point, we provide an upper bound on the MSPE of KALE and stochastic Kriging. The upper bound is close to zero if the noise is small, which implies the MSPE of KALE and stochastic Kriging are close. We also provide an asymptotic upper bound on the MSPE of KALE/KALEN and stochastic Kriging with estimated parameters. These results indicate that if the number of data points is large or the variance of the intrinsic noise is small, then there is not much difference between KALE/KALEN and stochastic Kriging in terms of prediction accuracy. The numeric results corroborate our theory. A case study is presented to illustrate the performance of KALEN and stochastic Kriging for modeling in the composite parts assembly process. In this paper, the MSPE of KALE, KALEN, and stochastic Kriging are primarily considered asymptotically. The theory does not cover the results under non-asymptotic cases. It can be expected that the difference between the MSPE of KALE/KALEN and stochastic Kriging will decrease as the fill distance decreases.

The calculation of the predictor (6) is not efficient if the integrals in (4) and (5) do not have an analytic form. If the sample size is large, then using pseudo maximum likelihood to estimate the unknown parameters is challenging, especially when the integrals in (4) and (5) do not have analytic forms. In this case, using stochastic Kriging as an alternative would be more desirable.

A A Lemma about MSPE of Stochastic Kriging

Lemma 2. *Assume Assumptions 1 and 2 are true. For any fixed constant $\mu > 0$, $\Psi(x, x) - \Psi(x, X)(\Psi(X, X) + \mu I)^{-1}\Psi(x, X)^T$ converges to zero as the fill distance of X goes to zero, where $\Psi(x, X)$ and $\Psi(X, X)$ are as in Theorem 2.*

Proof. Note $\Psi(x, x) - \Psi(x, X)(\Psi(X, X) + \mu I)^{-1}\Psi(x, X)^T \leq \|\Psi(\cdot, x) - \Psi(\cdot, X)^T(\Psi(X, X) + \mu I)^{-1}\Psi(x, X)^T\|_{L_\infty(\Omega)}$. Define $g(t) = \Psi(t, x) - \Psi(t, X)(\Psi(X, X) + \mu I)^{-1}\Psi(x, X)^T$. Under Assumption 1, we have $g \in H^2(\Omega)$, where $H^2(\Omega)$ is the Sobolev space. By the interpolation inequality, $\|g\|_{L_\infty(\Omega)} \leq C_1 \|g\|_{L_2(\Omega)}^{\frac{4}{4+d}} \|g\|_{H^2(\Omega)}^{\frac{d}{4+d}}$. By Corollary 10.25 in Wendland (2004) and

the fact that $\Psi(X, X)^{-1} \succeq (\Psi(X, X) + \mu I)^{-1}$, it can be shown that $\|g\|_{H^2(\Omega)} \leq C_2$. Thus, the result follows if we can show $\|g\|_{L_2(\Omega)}$ converges to zero. By the representer theorem, $\hat{g}_1(t) := \Psi(t, X)(\Psi(X, X) + \mu I)^{-1}\Psi(x, X)^T$ is the solution to the optimization problem

$$\min_{g_1 \in \mathcal{N}_\Psi(\Omega)} \frac{1}{n} \sum_{j=1}^n (g_1(x_j) - \Psi(x, x_j))^2 + \frac{\mu}{n} \|g_1\|_{\mathcal{N}_\Psi(\Omega)}^2, \quad (25)$$

where $\|\cdot\|_{\mathcal{N}_\Psi(\Omega)}$ is the norm of the reproducing kernel Hilbert space $\mathcal{N}_\Psi(\Omega)$. Under Assumption 2, by Lemma 3.4 of Utreras (1988), the result follows from

$$\begin{aligned} \|g\|_{L_2}^2 &\leq C_3 \left(\frac{1}{n} \sum_{j=1}^n (\hat{g}_1(x_j) - \Psi(x, x_j))^2 + h_X^4 \|g\|_{H^2(\Omega)}^2 \right) \\ &\leq C_3 \left(\frac{1}{n} \sum_{j=1}^n (\hat{g}_1(x_j) - \Psi(x, x_j))^2 + \frac{\mu}{n} \|g_1\|_{\mathcal{N}_\Psi(\Omega)}^2 + h_X^4 \|g\|_{H^2(\Omega)}^2 \right) \\ &\leq C_3 \left(\frac{1}{n} \sum_{j=1}^n (\Psi(x, x_j) - \Psi(x, x_j))^2 + \frac{\mu}{n} \|\Psi(x, \cdot)\|_{\mathcal{N}_\Psi(\Omega)}^2 + h_X^4 \|g\|_{H^2(\Omega)}^2 \right) \rightarrow 0, \end{aligned}$$

where the last inequality is true because \hat{g}_1 is the solution to (25). \square

B Proof of Lemma 1

By Fourier transform Wendland (2004), we have

$$\Psi(x_j, x_k) = \frac{1}{(2\pi)^d} \int_{\mathbb{R}^d} e^{i\langle x_j - x_k, t \rangle} \mathcal{F}(\Psi)(t) dt, \quad (26)$$

where $\langle s, t \rangle = s^T t$ is the inner product in \mathbb{R}^d . Therefore, direct calculation leads to

$$\begin{aligned} \Psi_S(x_j, x_k) &= \int_{\mathbb{R}^d} \int_{\mathbb{R}^d} \frac{1}{(2\pi)^d} \int_{\mathbb{R}^d} e^{i\langle x_j + \epsilon_1 - (x_k + \epsilon_2), t \rangle} \mathcal{F}(\Psi)(t) h(\epsilon_1) h(\epsilon_2) dt d\epsilon_1 d\epsilon_2 \\ &= \frac{1}{(2\pi)^d} \int_{\mathbb{R}^d} \left(\int_{\mathbb{R}^d} \int_{\mathbb{R}^d} e^{i\langle x_j + \epsilon_1 - (x_k + \epsilon_2), t \rangle} h(\epsilon_1) h(\epsilon_2) d\epsilon_1 d\epsilon_2 \right) \mathcal{F}(\Psi)(t) dt \\ &= \frac{1}{(2\pi)^d} \int_{\mathbb{R}^d} e^{i\langle x_j - x_k, t \rangle} \left(\int_{\mathbb{R}^d} e^{i\langle \epsilon_1, t \rangle} \int_{\mathbb{R}^d} e^{i\langle -\epsilon_2, t \rangle} h(\epsilon_1) h(\epsilon_2) d\epsilon_1 d\epsilon_2 \right) \mathcal{F}(\Psi)(t) dt \\ &= \frac{1}{(2\pi)^d} \int_{\mathbb{R}^d} e^{i\langle x_j - x_k, t \rangle} \left(\int_{\mathbb{R}^d} e^{i\langle -\epsilon_1, t \rangle} h(\epsilon_1) d\epsilon_1 \right) \left(\int_{\mathbb{R}^d} e^{i\langle \epsilon_2, t \rangle} h(\epsilon_2) d\epsilon_2 \right) \mathcal{F}(\Psi)(t) dt. \end{aligned} \quad (27)$$

For any $w = (w_1, \dots, w_n)^T$, by (27), we have

$$\begin{aligned} & \sum_{j,k=1}^n w_j \bar{w}_k \Psi_S(x_j, x_k) \\ &= \sum_{j,k=1}^n w_j \bar{w}_k \frac{1}{(2\pi)^d} \int_{\mathbb{R}^d} e^{i\langle x_j - x_k, t \rangle} \left(\int_{\mathbb{R}^d} e^{i\langle -\epsilon_1, t \rangle} h(\epsilon_1) d\epsilon_1 \right) \left(\int_{\mathbb{R}^d} e^{i\langle \epsilon_2, t \rangle} h(\epsilon_2) d\epsilon_2 \right) \mathcal{F}(\Psi)(t) dt \\ &= \frac{1}{(2\pi)^d} \int_{\mathbb{R}^d} \left| \sum_{j=1}^n w_j e^{i\langle x_j, t \rangle} \right|^2 \left(1 - \left(\int_{\mathbb{R}^d} e^{i\langle -\epsilon_1, t \rangle} h(\epsilon_1) d\epsilon_1 \right) \left(\int_{\mathbb{R}^d} e^{i\langle \epsilon_2, t \rangle} h(\epsilon_2) d\epsilon_2 \right) \right) \mathcal{F}(\Psi)(t) dt. \end{aligned}$$

Let

$$c(t) = \left(\int_{\mathbb{R}^d} e^{i\langle -\epsilon_1, t \rangle} h(\epsilon_1) d\epsilon_1 \right) \left(\int_{\mathbb{R}^d} e^{i\langle \epsilon_2, t \rangle} h(\epsilon_2) d\epsilon_2 \right).$$

Thus, $c(t) \in \mathbb{R}$. Since $|e^{i\langle -\epsilon_1, t \rangle}| \leq 1$, $c(t) \leq 1$. Therefore, $\sum_{j,k=1}^n w_j \bar{w}_k \Psi_S(x_j, x_k) \geq 0$, which finishes the proof.

C Proof of Theorem 1

Consider the following Gaussian process with extrinsic error,

$$y_S(x) = M_S(x) + \delta(x), \quad (28)$$

where M_S is a mean zero Gaussian process with covariance function $\sigma^2 \Psi_S(\cdot, \cdot)$, and $\delta(x)$ is an independent noise process with mean zero and variance μ . The best linear unbiased predictor of (28) is

$$\hat{f}_S(x) = r_N(x)^T (K_S + \mu I_n)^{-1} Y, \quad (29)$$

and the MSPE is

$$\text{MSPE}_S = \sigma^2 \Psi_S(x, x) - r_N(x)^T (K_S + \mu I_n)^{-1} r_N(x). \quad (30)$$

By Lemma 2, (30) goes to zero as the fill distance of X goes to zero.

Take $\mu = \sigma^2(\Psi(x, x) - \Psi_S(x, x))$. It can be seen that (30) is equal to $\sigma^2 \Psi_S(x, x) - r_N(x) K^{-1} r_N(x)$. By (10), $\mathbb{E}(y(x) - \hat{y}(x))^2 = \text{MSPE}_S + \sigma^2(\Psi(x, x) - \Psi_S(x, x))$, which converges to $\sigma^2(\Psi(x, x) - \Psi_S(x, x))$ as the fill distance of the design points goes to zero. This completes the proof.

D Proof of Proposition 1

Without loss of generality, assume $\sigma = 1$.

Let K_1 and K_2 be the kernel matrix corresponding to the kernel functions $\Psi_1(x_i, x_j) = \exp\left(\frac{-\theta \|x_i - x_j\|^2}{1 + 4\sigma_1^2 \theta}\right)$ and $\Psi_2(x_i, x_j) = \exp\left(\frac{-\theta \|x_i - x_j\|^2}{1 + 2\sigma_1^2 \theta}\right)$, respectively. Therefore, $K = \frac{1}{(1 + 4\sigma_1^2 \theta)^{d/2}} K_1 +$

$(1 - \frac{1}{(1+4\sigma_1^2\theta)^{d/2}})I_n$. Plugging in r and substituting K with $\frac{1}{(1+4\sigma_1^2\theta)^{d/2}}K_1 + (1 - \frac{1}{(1+4\sigma_1^2\theta)^{d/2}})I_n$, we have

$$1 - r(x)^T K^{-1} r(x) = 1 - \frac{(1 + 4\sigma_1^2\theta)^{d/2}}{(1 + 2\sigma_1^2\theta)^d} r_2(X)(K_1 + aI)^{-1} r_2(x), \quad (31)$$

where $a = (1 + 4\sigma_1^2\theta)^{d/2} - 1$ and $r_2(x) = (r_2(x, x_1), \dots, r_2(x, x_n))^T$ with

$$r_2(x, x_i) = e^{-\frac{\theta\|x-x_i\|^2}{1+2\sigma_1^2\theta}}.$$

Note that $\Psi_2(s, t) \leq \Psi_1(s, t)$ for any $s, t \in \Omega$, by Paulsen and Raghupathi (2016), $\mathcal{N}_{\Psi_2}(\Omega) \subset \mathcal{N}_{\Psi_1}(\Omega)$ and $K_2 \preceq K_1$. Therefore, the MSPE of KALE is lower bounded by

$$\begin{aligned} 1 - r(x)^T K^{-1} r(x) &= 1 - \frac{(1 + 4\sigma_1^2\theta)^{d/2}}{(1 + 2\sigma_1^2\theta)^d} r_2(x)(K_1 + aI)^{-1} r_2(x) \\ &\geq 1 - \frac{(1 + 4\sigma_1^2\theta)^{d/2}}{(1 + 2\sigma_1^2\theta)^d} + \frac{(1 + 4\sigma_1^2\theta)^{d/2}}{(1 + 2\sigma_1^2\theta)^d} \left(1 - r_2(x)(K_2 + aI)^{-1} r_2(x)\right). \end{aligned}$$

Noting that $1 - r_2(x)(K_2 + aI)^{-1} r_2(x)$ is the MSPE of the Gaussian process with kernel function Ψ_2 with a constant nugget parameter, it converges to zero as the fill distance goes to zero by Lemma 2. Furthermore, $1 - r_2(x)(K_2 + aI)^{-1} r_2(x) > 0$. Therefore, the MSPE of KALE is lower bounded by $1 - \frac{(1+4\sigma_1^2\theta)^{d/2}}{(1+2\sigma_1^2\theta)^d}$.

E Proof of Theorem 2

Without loss of generality, assume $\sigma = 1$. First, we consider there is noise at an untried point. For any $u = (u_1, \dots, u_n)^T$, it can be shown that the MSPE of predictor $u^T Y$ is

$$\begin{aligned} &\mathbb{E} \left\| \Psi(\cdot, x + \epsilon) - \sum_{i=1}^n u_i \Psi(\cdot, x_i + \epsilon) \right\|_{\mathcal{N}_{\Psi}}^2 \\ &= \Psi(x, x) - 2 \sum_{j=1}^n u_j \Psi_S(x, x_j) + \sum_{j,k=1}^n u_j u_k \Psi_S(x_j, x_k) + a \|u\|_2^2, \end{aligned} \quad (32)$$

where $\|\cdot\|_{\mathcal{N}_{\Psi}(\Omega)}$ is the norm of the reproducing kernel Hilbert space $\mathcal{N}_{\Psi}(\Omega)$ and $a = \Psi(x, x) - \Psi_S(x, x)$. Notice that

$$\Psi_S(x_j, x_k) = \frac{1}{(2\pi)^d} \int_{\mathbb{R}^d} e^{i\langle x_j - x_k, t \rangle} c(t) \mathcal{F}(\Psi)(t) dt,$$

where

$$c(t) = \left(\int_{\mathbb{R}^d} e^{i\langle -\epsilon_j, t \rangle} h(\epsilon_j) d\epsilon_j \right) \left(\int_{\mathbb{R}^d} e^{i\langle \epsilon_k, t \rangle} h(\epsilon_k) d\epsilon_k \right).$$

Since $|e^{i\langle -\epsilon_j, t \rangle}| \leq 1$, $c(t) \leq 1$. Therefore, (32) can be bounded by

$$\begin{aligned}
& \Psi(x, x) - 2 \sum_{j=1}^n u_j \Psi_S(x, x_j) + \sum_{j,k=1}^n u_j u_k \Psi_S(x_j, x_k) + a \|u\|_2^2 \\
&= u^T \Psi_S(X, X) u - 2u^T \Psi_S(X, x) + \Psi_S(x, x) + a \|u\|_2^2 + a \\
&= \frac{1}{(2\pi)^d} \int_{\mathbb{R}^d} \left| \sum_{j=1}^n u_j e^{i\langle x_j, t \rangle} - e^{i\langle x, t \rangle} \right|^2 c(t) \mathcal{F}(\Psi)(t) dt + a \|u\|_2^2 + a \\
&\leq \frac{1}{(2\pi)^d} \int_{\mathbb{R}^d} \left| \sum_{j=1}^n u_j e^{i\langle x_j, t \rangle} - e^{i\langle x, t \rangle} \right|^2 \mathcal{F}(\Psi)(t) dt + a \|u\|_2^2 + a \\
&= u^T \Psi(X, X) u - 2u^T \Psi(X, x) + \Psi(x, x) + a \|u\|_2^2 + a \\
&\leq \max\{1, a/\mu\} (u^T \Psi(X, X) u - 2u^T \Psi(X, x) + \Psi(x, x) + \mu \|u\|_2^2) + a. \tag{33}
\end{aligned}$$

Plugging

$$u = (\Psi(X, X) + \mu I)^{-1} \Psi(X, x),$$

into (32) and (33), we have the MSPE of predictor (14) upper bounded by

$$\max\{1, a/\mu\} (\Psi(x, x) - \Psi(x, X) (\Psi(X, X) + \mu I)^{-1} \Psi(X, x)) + a.$$

By Lemma 2, $\Psi(x, x) - \Psi(x, X) (\Psi(X, X) + \mu I)^{-1} \Psi(X, x)$ goes to zero as the fill distance goes to zero since μ is a constant, which completes the proof in this case.

Next, we consider the case that there is no noise at an untried point. For any $u = (u_1, \dots, u_n)^T$, it can be shown that the MSPE of predictor $u^T Y$ in this case is

$$\begin{aligned}
& \mathbb{E} \left\| \Psi(\cdot, x) - \sum_{j=1}^n u_j \Psi(\cdot, x_j + \epsilon) \right\|_{\mathcal{N}_\Psi}^2 \\
&= u^T \Psi_S(X, X) u - 2u^T r(x) + \Psi(x, x) + a \|u\|_2^2. \tag{34}
\end{aligned}$$

Let $b(t) = \int_{\mathbb{R}^d} e^{i\langle \epsilon_i, t \rangle} h(\epsilon_i) d\epsilon_i$. Thus, for any $u = (u_1, \dots, u_n)^T$, we have

$$\begin{aligned}
& u^T \Psi_S(X, X) u - 2u^T r(x) + \Psi(x, x) + a \|u\|_2^2 \\
&= \frac{1}{(2\pi)^d} \int_{\mathbb{R}^d} \left| \sum_{j=1}^n u_j e^{i\langle x_j, t \rangle} b(t) - e^{i\langle x, t \rangle} \right|^2 \mathcal{F}(\Psi)(t) dt + a \|u\|_2^2 \\
&\leq \frac{2}{(2\pi)^d} \int_{\mathbb{R}^d} \left| \sum_{j=1}^n u_j e^{i\langle x_j, t \rangle} - e^{i\langle x, t \rangle} \right|^2 |b(t)|^2 \mathcal{F}(\Psi)(t) dt + \frac{2}{(2\pi)^d} \int_{\mathbb{R}^d} |1 - |b(t)||^2 \mathcal{F}(\Psi)(t) dt + a \|u\|_2^2 \\
&= 2(u^T \Psi(X, X) u - 2u^T \Psi(X, x) + \Psi(x, x)) + a \|u\|_2^2 + \frac{2}{(2\pi)^d} \int_{\mathbb{R}^d} |1 - |b(t)||^2 \mathcal{F}(\Psi)(t) dt \\
&\leq \max\{2, a/\mu\} (u^T \Psi(X, X) u - 2u^T \Psi(X, x) + \Psi(x, x) + \mu \|u\|_2^2) + \frac{2}{(2\pi)^d} \int_{\mathbb{R}^d} |1 - |b(t)||^2 \mathcal{F}(\Psi)(t) dt. \tag{35}
\end{aligned}$$

Plugging

$$u = (\Psi(X, X) + \mu I)^{-1} \Psi(X, x),$$

into (34) and (35), we have the MSPE of predictor (14) upper bounded by

$$\max\{2, a/\mu\}(\Psi(x, x) - \Psi(x, X)(\Psi(X, X) + \mu I)^{-1} \Psi(X, x)) + \frac{2}{(2\pi)^d} \int_{\mathbb{R}^d} |1 - |b(t)||^2 |\mathcal{F}(\Psi)(t)| dt.$$

By Lemma 2, $\Psi(x, x) - \Psi(x, X)(\Psi(X, X) + \mu I)^{-1} \Psi(X, x)$ goes to zero as the fill distance goes to zero since μ is a constant, which finishes the proof in this case.

F Proof of Proposition 2

Notice that $E(e^{i\epsilon_n^T t})$ converges to 1 since ϵ_n converges to 0 in distribution and $e^{i\epsilon_n^T t}$ is bounded, and $b(t)$ is bounded for all $t \in \mathbb{R}^d$. By dominated convergence theorem, the result holds.

G Proof of Theorem 3

We first present a lemma, which is a generalization of Lemma 2.

Lemma 3. *Suppose the conditions of Theorem 3 hold. Then we have $\Psi(x, x) - \hat{\Psi}(x, X)(\hat{\Psi}(X, X) + \hat{\mu}I)^{-1} \hat{\Psi}(x, X)^T$ converges to zero as the fill distance of X converges to zero.*

Proof. The proof of Lemma 3 is similar to the proof of Lemma 2. The only difference is that if we define $\hat{g}(t) = \hat{\Psi}(t, x) - \hat{\Psi}(t, X)(\hat{\Psi}(X, X) + \hat{\mu}I)^{-1} \hat{\Psi}(x, X)^T$, then $\|\hat{g}\|_{H^2(\Omega)} \leq C_2$ for all \hat{g} . Thus, the result follows from the proof of Lemma 2. \square

Now we are ready to show the proof of Theorem 3. Let $\tilde{y}(x)$ be the stochastic Kriging predictor with estimated parameters $(\hat{\theta}_2, \hat{\mu})$. Thus,

$$\tilde{y}(x) = \hat{\Psi}_2(x, X)(\hat{\Psi}_2(X, X) + \hat{\mu}I)^{-1} Y, \quad (36)$$

where $\hat{\Psi}_2(x, X) = (\hat{\Psi}_2(x, x_1), \dots, \hat{\Psi}_2(x, x_n))$ and $\hat{\Psi}_2(X, X) = (\hat{\Psi}_2(x_j, x_k))_{jk}$. Because KALE and KALEN are best linear unbiased predictors, i.e., have the smallest MSPE among all linear predictors, and $\tilde{y}(x)$ is a linear predictor, it suffices to show the upper bounds hold for the stochastic Kriging predictor \tilde{y} .

Proof of Statement (i):

Direct calculation shows that the MSPE can be expressed as

$$\begin{aligned} \mathbb{E}(y(x) - \tilde{y}(x))^2 &= \sigma^2(\Psi(x, x) - 2\hat{\Psi}_2(x, X)(\hat{\Psi}_2(X, X) + \hat{\mu}I)^{-1} r_N(x) \\ &\quad + \hat{\Psi}_2(x, X)(\hat{\Psi}_2(X, X) + \hat{\mu}I)^{-1} K(\hat{\Psi}_2(X, X) + \hat{\mu}I)^{-1} \hat{\Psi}_2(x, X)^T), \end{aligned} \quad (37)$$

where K and r_N are as in (5) and (7), respectively. Similar to (33), we have for any $u = (u_1, \dots, u_n)^T$,

$$\begin{aligned}
& \Psi(x, x) - 2 \sum_{j=1}^n u_j \Psi_S(x, x_j) + \sum_{j,k=1}^n u_j u_k \Psi_S(x_j, x_k) + a \|u\|_2^2 \\
&= u^T \Psi_S(X, X) u - 2u^T \Psi_S(X, x) + \Psi_S(x, x) + a \|u\|_2^2 + a \\
&= \frac{1}{(2\pi)^d} \int_{\mathbb{R}^d} \left| \sum_{j=1}^n u_j e^{i\langle x_j, t \rangle} - e^{i\langle x, t \rangle} \right|^2 c(t) \mathcal{F}(\Psi)(t) dt + a \|u\|_2^2 + a \\
&\leq \frac{1}{(2\pi)^d} \int_{\mathbb{R}^d} \left| \sum_{j=1}^n u_j e^{i\langle x_j, t \rangle} - e^{i\langle x, t \rangle} \right|^2 \mathcal{F}(\Psi)(t) dt + a \|u\|_2^2 + a \\
&\leq \frac{A_1}{(2\pi)^d} \int_{\mathbb{R}^d} \left| \sum_{j=1}^n u_j e^{i\langle x_j, t \rangle} - e^{i\langle x, t \rangle} \right|^2 \mathcal{F}(\hat{\Psi}_2)(t) dt + a \|u\|_2^2 + a \\
&= A_1 (u^T \hat{\Psi}_2(X, X) u - 2u^T \hat{\Psi}_2(X, x) + \hat{\Psi}_2(x, x)) + a \|u\|_2^2 + a \\
&\leq \max\{A_1, a/\hat{\mu}\} (u^T \hat{\Psi}_2(X, X) u - 2u^T \hat{\Psi}_2(X, x) + \hat{\Psi}_2(x, x) + \hat{\mu} \|u\|_2^2) + a, \tag{38}
\end{aligned}$$

where

$$c(t) = \left(\int_{\mathbb{R}^d} e^{i\langle -\epsilon_j, t \rangle} h(\epsilon_j) d\epsilon_j \right) \left(\int_{\mathbb{R}^d} e^{i\langle \epsilon_k, t \rangle} h(\epsilon_k) d\epsilon_k \right),$$

and $a = \Psi(x, x) - \Psi_S(x, x)$. Plugging

$$u = (\hat{\Psi}_2(X, X) + \hat{\mu}I)^{-1} \hat{\Psi}_2(X, x),$$

into (37) and (38), we have the MSPE of predictor (37) is upper bounded by

$$\begin{aligned}
& \max\{A_1, a/\hat{\mu}\} (\hat{\Psi}_2(x, x) - \hat{\Psi}_2(x, X) (\hat{\Psi}_2(X, X) + \hat{\mu}I)^{-1} \hat{\Psi}_2(X, x)) + a \\
&\leq \max\{A_1, aC\} (\hat{\Psi}_2(x, x) - \hat{\Psi}_2(x, X) (\hat{\Psi}_2(X, X) + CI)^{-1} \hat{\Psi}_2(X, x)) + a
\end{aligned}$$

By Lemma 3, $\hat{\Psi}_2(x, x) - \hat{\Psi}_2(x, X) (\hat{\Psi}_2(X, X) + CI)^{-1} \hat{\Psi}_2(X, x)$ goes to zero as the fill distance goes to zero, which indicates that $\sigma^2 a$ is an asymptotic upper bound on the MSPE of KALEN and stochastic Kriging with estimated parameters. Note that $\sigma^2 a$ is also the limit of KALEN with the true parameters, which is the best linear unbiased predictor. Therefore, $\sigma^2 a$ is the limit of KALEN and stochastic Kriging with estimated parameters, which completes the proof of Statement (i).

Proof of Statement (ii):

By direct calculation, it can be shown that

$$\begin{aligned}
\mathbb{E}(y(x) - \tilde{y}(x))^2 &= \sigma^2 (\Psi(x, x) - 2\hat{\Psi}_2(x, X) (\hat{\Psi}_2(X, X) + \hat{\mu}I)^{-1} r(x) \\
&\quad + \hat{\Psi}_2(x, X) (\hat{\Psi}_2(X, X) + \hat{\mu}I)^{-1} K (\hat{\Psi}_2(X, X) + \hat{\mu}I)^{-1} \hat{\Psi}_2(X, x)), \tag{39}
\end{aligned}$$

where $r(x)$ is as in (4). Let $b(t) = \int_{\mathbb{R}^d} e^{i\langle \epsilon_j, t \rangle} h(\epsilon_j) d\epsilon_j$. Similar to (35), for any $u = (u_1, \dots, u_n)^T$, we have

$$\begin{aligned}
& u^T \Psi_S(X, X)u - 2u^T r(x) + \Psi(x, x) + a\|u\|_2^2 \\
&= \frac{1}{(2\pi)^d} \int_{\mathbb{R}^d} \left| \sum_{j=1}^n u_j e^{i\langle x_j, t \rangle} b(t) - e^{i\langle x, t \rangle} \right|^2 \mathcal{F}(\Psi)(t) dt + a\|u\|_2^2 \\
&\leq \frac{2}{(2\pi)^d} \int_{\mathbb{R}^d} \left| \sum_{j=1}^n u_j e^{i\langle x_j, t \rangle} - e^{i\langle x, t \rangle} \right|^2 |b(t)|^2 \mathcal{F}(\Psi)(t) dt + \frac{2}{(2\pi)^d} \int_{\mathbb{R}^d} |1 - |b(t)||^2 \mathcal{F}(\Psi)(t) dt + a\|u\|_2^2 \\
&\leq \frac{2A_1}{(2\pi)^d} \int_{\mathbb{R}^d} \left| \sum_{j=1}^n u_j e^{i\langle x_j, t \rangle} - e^{i\langle x, t \rangle} \right|^2 |b(t)|^2 \mathcal{F}(\hat{\Psi}_2)(t) dt + \frac{2}{(2\pi)^d} \int_{\mathbb{R}^d} |1 - |b(t)||^2 \mathcal{F}(\Psi)(t) dt + a\|u\|_2^2 \\
&= 2A_1(u^T \hat{\Psi}_2(X, X)u - 2u^T \hat{\Psi}_2(X, s) + \hat{\Psi}_2(x, x)) + a\|u\|_2^2 + \frac{2}{(2\pi)^d} \int_{\mathbb{R}^d} |1 - |b(t)||^2 \mathcal{F}(\Psi)(t) dt \\
&\leq \max\{2A_1, a/\hat{\mu}\}(u^T \hat{\Psi}_2(X, X)u - 2u^T \hat{\Psi}_2(X, x) + \hat{\Psi}_2(x, x) + \hat{\mu}\|u\|_2^2) + \frac{2}{(2\pi)^d} \int_{\mathbb{R}^d} |1 - |b(t)||^2 \mathcal{F}(\Psi)(t) dt.
\end{aligned} \tag{40}$$

Plugging

$$u = (\hat{\Psi}_2(X, X) + \hat{\mu}I)^{-1} \hat{\Psi}_2(X, x),$$

into (39) and (40), we find the MSPE of predictor (14) is upper bounded by

$$\begin{aligned}
& \max\{2A_1, a/\hat{\mu}\}(\hat{\Psi}_2(x, x) - \hat{\Psi}_2(x, X)(\hat{\Psi}_2(X, X) + \hat{\mu}I)^{-1} \hat{\Psi}_2(X, x)) + \frac{2}{(2\pi)^d} \int_{\mathbb{R}^d} |1 - |b(t)||^2 \mathcal{F}(\Psi)(t) dt \\
&\leq \max\{2A_1, aC\}(\hat{\Psi}_2(x, x) - \hat{\Psi}_2(x, X)(\hat{\Psi}_2(X, X) + CI)^{-1} \hat{\Psi}_2(X, x)) + \frac{2}{(2\pi)^d} \int_{\mathbb{R}^d} |1 - |b(t)||^2 \mathcal{F}(\Psi)(t) dt.
\end{aligned}$$

By Lemma 3, $\hat{\Psi}(x, x) - \hat{\Psi}(x, X)(\hat{\Psi}(X, X) + CI)^{-1} \hat{\Psi}(X, x)$ converges to zero as the fill distance goes to zero since C is a constant, which finishes the proof of Statement (ii).

References

- Ankenman, B., Nelson, B. L., and Staum, J. (2010). Stochastic kriging for simulation metamodeling. *Operations Research*, 58(2):371–382.
- Barber, J. J., Gelfand, A. E., and Silander, J. A. (2006). Modelling map positional error to infer true feature location. *Canadian Journal of Statistics*, 34(4):659–676.
- Bócsi, B. A. and Csató, L. (2013). Hessian corrected input noise models. In *International Conference on Artificial Neural Networks*, pages 1–8. Springer.
- Cervone, D. and Pillai, N. S. (2015). Gaussian process regression with location errors. *arXiv preprint arXiv:1506.08256*.

- Cressie, N. (2015). *Statistics for Spatial Data*. John Wiley & Sons.
- Cressie, N. and Kornak, J. (2003). Spatial statistics in the presence of location error with an application to remote sensing of the environment. *Statistical Science*, 18(4):436–456.
- Dallaire, P., Besse, C., and Chaib-Draa, B. (2009). Learning Gaussian process models from uncertain data. In *International Conference on Neural Information Processing*, pages 433–440. Springer.
- Deisenroth, M. P., Fox, D., and Rasmussen, C. E. (2015). Gaussian processes for data-efficient learning in robotics and control. *IEEE Transactions on Pattern Analysis and Machine Intelligence*, 37(2):408–423.
- Fang, K.-T., Li, R., and Sudjianto, A. (2005). *Design and Modeling for Computer Experiments*. CRC Press.
- Girard, A. (2004). *Approximate Methods for Propagation of Uncertainty with Gaussian Process Models*. Ph.D. thesis, University of Glasgow.
- Halton, J. H. (1964). Algorithm 247: Radical-inverse quasi-random point sequence. *Communications of the ACM*, 7(12):701–702.
- He, S., Lin, W., and Chan, S.-H. G. (2017). Indoor localization and automatic fingerprint update with altered ap signals. *IEEE Transactions on Mobile Computing*, 16(7):1897–1910.
- Higdon, D. (2002). Space and space-time modeling using process convolutions. In *Quantitative Methods for Current Environmental Issues*, pages 37–56. Springer.
- Lim, Y. B., Sacks, J., Studden, W., and Welch, W. J. (2002). Design and analysis of computer experiments when the output is highly correlated over the input space. *Canadian Journal of Statistics*, 30(1):109–126.
- Matheron, G. (1963). Principles of geostatistics. *Economic Geology*, 58(8):1246–1266.
- McHutchon, A. and Rasmussen, C. E. (2011). Gaussian process training with input noise. In *Advances in Neural Information Processing Systems*, pages 1341–1349.
- Muppirisetty, L. S., Svensson, T., and Wymeersch, H. (2016). Spatial wireless channel prediction under location uncertainty. *IEEE Transactions on Wireless Communications*, 15(2):1031–1044.
- Paulsen, V. I. and Raghupathi, M. (2016). *An Introduction to the Theory of Reproducing Kernel Hilbert Spaces*, volume 152. Cambridge University Press.
- Sacks, J., Welch, W. J., Mitchell, T. J., and Wynn, H. P. (1989). Design and analysis of computer experiments. *Statistical Science*, 4:409–423.
- Santner, T. J., Williams, B. J., and Notz, W. I. (2013). *The Design and Analysis of Computer Experiments*. Springer Science & Business Media.

- Stein, M. L. (1999). *Interpolation of Spatial Data: Some Theory for Kriging*. Springer Science & Business Media.
- Utreras, F. I. (1988). Convergence rates for multivariate smoothing spline functions. *Journal of approximation theory*, 52(1):1–27.
- Veneziano, D. and Van Dyck, J. (1987). Statistical analysis of earthquake catalogs for seismic hazard. In *Stochastic Approaches in Earthquake Engineering*, pages 385–427. Springer.
- Wang, W., Tuo, R., and Wu, C. J. (2019). On prediction properties of kriging: Uniform error bounds and robustness. *Journal of the American Statistical Association*, (just-accepted).
- Wen, Y., Yue, X., Hunt, J. H., and Shi, J. (2018). Feasibility analysis of composite fuselage shape control via finite element analysis. *Journal of Manufacturing Systems*, 46:272–281.
- Wendland, H. (2004). *Scattered Data Approximation*, volume 17. Cambridge University Press.
- Wu, C. F. J. and Hamada, M. S. (2009). *Experiments: Planning, Analysis, and Optimization*. John Wiley & Sons, 2nd edition.
- Ying, Z. (1991). Asymptotic properties of a maximum likelihood estimator with data from a Gaussian process. *Journal of Multivariate Analysis*, 36(2):280–296.
- Yue, X., Wen, Y., Hunt, J. H., and Shi, J. (2018). Surrogate model based control considering uncertainty for composite fuselage assembly. *ASME Transactions, Journal of Manufacturing Science and Engineering*, 140(4):041017.
- Zhang, H. (2004). Inconsistent estimation and asymptotically equal interpolations in model-based geostatistics. *Journal of the American Statistical Association*, 99(465):250–261.